



HAL
open science

Effects of elevated ozone concentration and nitrogen addition on ammonia stomatal compensation point in a poplar clone

Wen Xu, Bo Shang, Yansen Xu, Xiangyang Yuan, Anthony J Dore, Yuanhong Zhao, Raia-Silvia Massad, Zhaozhong Feng

► To cite this version:

Wen Xu, Bo Shang, Yansen Xu, Xiangyang Yuan, Anthony J Dore, et al.. Effects of elevated ozone concentration and nitrogen addition on ammonia stomatal compensation point in a poplar clone. *Environmental Pollution*, 2018, 238, pp.760-770. 10.1016/j.envpol.2018.03.089 . hal-04353491

HAL Id: hal-04353491

<https://hal.science/hal-04353491v1>

Submitted on 19 Dec 2023

HAL is a multi-disciplinary open access archive for the deposit and dissemination of scientific research documents, whether they are published or not. The documents may come from teaching and research institutions in France or abroad, or from public or private research centers.

L'archive ouverte pluridisciplinaire **HAL**, est destinée au dépôt et à la diffusion de documents scientifiques de niveau recherche, publiés ou non, émanant des établissements d'enseignement et de recherche français ou étrangers, des laboratoires publics ou privés.

Public Domain

1 MS Number: ENVPOL_2018_333_R1

2 **Effects of elevated ozone concentration and fertilization on ammonia stomatal**
3 **compensation point in a poplar clone**

4 Wen Xu^{1,2}, Bo Shang^{1,2}, Yansen Xu^{1,2}, Xiangyang Yuan^{1,2}, Anthony J. Dore³, Yuanhong
5 Zhao⁴, Raia-Silvia Massad⁵, Zhaozhong Feng^{1,2*}

6

7 ¹State Key Laboratory of Urban and Regional Ecology, Research Center for Eco-
8 Environmental Sciences, Chinese Academy of Sciences, Shuangqing Road 18, Haidian
9 District, Beijing 100085, China.

10 ²College of Resources and Environment, University of Chinese Academy of Sciences,
11 Beijing 100049, China.

12 ³Centre for Ecology and Hydrology, Edinburgh, Bush Estate, Penicuik, Midlothian
13 EH26 0QB, UK.

14 ⁴Laboratory for Climate and Ocean-Atmosphere Sciences, Department of Atmospheric
15 and Oceanic Sciences, School of Physics, Peking University, Beijing100871, China.

16 ⁵ UMR ECOSYS, INRA, Agroparistech, Université Paris-Saclay Thiverval-Grignon
17 France.

18 *Corresponding author.

19 E-mail address: fzz@rcees.ac.cn (Z. Feng).

20 **Abstract:** The stomatal compensation point of ammonia (χ_s) is a key factor controlling
21 plant-atmosphere NH_3 exchange, which is dependent on the nitrogen (N) supply and
22 varies among plant species. However, knowledge gaps remain concerning the effects
23 of elevated atmospheric N deposition and ozone (O_3) on χ_s for forest species, resulting
24 in large uncertainties in the parameterizations of NH_3 incorporated into atmospheric
25 chemistry and transport models (CTMs). Here, we present leaf-scale measurements of
26 χ_s for hybrid poplar clone ‘546’ (*Populus deltoides* cv. 55/56 x *P. deltoides* cv. Imperial)
27 growing in two N treatments (N0, no N added; N50, 50 kg N ha⁻¹ yr⁻¹ urea fertilizer
28 added) and two O_3 treatments (CF, charcoal-filtered air; E- O_3 , non-filtered air plus 40
29 ppb) for 105 days. Our results showed that χ_s was significantly reduced by E- O_3 (41%)
30 and elevated N (19%). The interaction of N and O_3 were significant, and N can mitigate
31 the negative effects of O_3 on χ_s . Elevated O_3 significantly reduced the light-saturated
32 photosynthetic rate (A_{sat}) and chlorophyll (Chl) content and significantly increased
33 intercellular CO_2 concentrations (C_i), but had no significant effect on stomatal
34 conductance (g_s). By contrast, elevated N did not significantly affect all measured
35 photosynthetic parameters. Overall, χ_s was significantly and positively correlated with
36 A_{sat} , g_s and Chl, whereas a significant and negative relationship was observed between
37 χ_s and C_i . Our results suggest that O_3 -induced changes in A_{sat} , C_i and Chl may affect χ_s .
38 Our findings provide a scientific basis for optimizing parameterizations of χ_s in
39 atmospheric chemistry and transport models to respond to environmental change
40 factors (i.e., elevated N deposition and/or O_3) in the future.

41 **Keywords:** Ammonia; Ozone; Apoplast; Compensation point; Forest species

42 **Capsule:** Both elevated O_3 and fertilization can significantly reduced NH_3 stomatal
43 compensation point (χ_s) of poplar clone ‘546’, and fertilization can mitigate the negative
44 effects of O_3 on χ_s .

45

46 1. Introduction

47 Atmospheric ammonia (NH_3) is the primary alkaline trace gas in the atmosphere
48 and plays a vital role in many biogeochemical and atmospheric processes (Behera et al.,
49 2013). It neutralizes atmospheric acids to yield ammonium (NH_4^+) aerosols,

50 which results in increased mass loadings of fine atmospheric particulate matter (PM_{2.5},
51 aerodynamic diameter ≤ 2.5) (Xu et al., 2016, 2017), thereby reducing visibility and
52 adversely impacting ecosystem and human health (Gu et al., 2014). By contrast,
53 atmospheric deposition of reduced N (NH₃ and NH₄⁺) can cause soil acidification (Du
54 et al., 2015), eutrophication (Pareman et al., 2016) and loss of biodiversity (Erisman et
55 al., 2007) in sensitive ecosystems.

56 Plants can be either a source or a sink of atmospheric NH₃, depending on the
57 difference between atmospheric NH₃ concentration and the so-called canopy NH₃
58 compensation point (Massad et al., 2010). As a major component of canopy NH₃
59 compensation point, ammonia stomatal compensation point (χ_s) is defined as the
60 atmospheric NH₃ concentration for which there is no exchange between the leaf and the
61 atmosphere under dry conditions (Flechard et al., 2013). Theoretically, χ_s is also the
62 gaseous NH₃ concentration in the leaf sub-stomatal cavity that is in equilibrium with
63 ammonium concentration in the apoplast (Husted and Schjoerring, 1995). It plays a
64 vital role in controlling the magnitude and the direction of NH₃ exchange between the
65 canopy and the atmosphere (Sutton et al., 1995). Specifically, if atmospheric NH₃
66 concentrations exceed χ_s then NH₃ deposition from the atmosphere to vegetation will
67 occur, while with atmospheric NH₃ concentrations below χ_s , there will be a net emission
68 of NH₃ by plants. χ_s depends directly on the plant nitrogen (N) status, developmental
69 stage, and environmental conditions (e.g., N fertilization), with larger values generally
70 observed under conditions of high N supply to the soil-plant system and at senescence
71 (Massad et al., 2009; Schjoerring et al., 1998).

72 χ_s can be derived from simultaneous measurement of vertical fluxes and
73 concentrations of NH₃ by using micrometeorological flux techniques over large fields
74 (Hansen et al., 2017; Nemitz et al., 2001; Personne et al., 2015), or in chambers by
75 finding the concentration at which the total flux is zero (Hill et al., 2001; Massad et al.,
76 2009; Wang et al., 2011). In addition, the bioassay approach has also been developed
77 for assessing χ_s and it is based on the determination of the leaf apoplastic NH₄⁺
78 concentration and pH by means of apoplast extraction (Husted and Schjoerring, 1995).
79 These two methods are complementary. Apoplast extraction is more appropriate for leaf

80 and cell scale processes whereas chamber/micrometeorological measurements tend to
81 be more appropriate for flux measurements at an entire plant/canopy scale (Massad et
82 al., 2009; Sutton et al., 2009).

83 Forests represent a major uncertainty in quantification of regional NH₃ fluxes and
84 parameterization of bi-directional NH₃ exchange in atmospheric chemistry and
85 transport models (CTMs) such as AURAMS (A Unified Regional Air-quality
86 Modelling System, Zhang et al., 2010) and CMAQ (Community Multiscale Air-Quality
87 Modeling System, Fu et al., 2015). This is not only due to the large land area of forests
88 but also because of the wide range of forest types and management practices. In
89 conditions of bi-directional NH₃ exchange, forests are of particular interest. For
90 example, temperate deciduous forests are potentially a natural source of NH₃ (Hansen
91 et al., 2013, 2017; Neirynek and Ceulemans, 2008), leading to impact of forests on the
92 atmospheric NH₃ level. In contrast, tropical humid forest and temperate coniferous
93 forest can acts as net NH₃ sinks (Bertolini et al., 2016; Duyzer et al., 2005), resulting in
94 the impact of atmospheric NH₃ on the ecological functioning of forests.

95 χ_s is one of the key parameters for parameterizations of NH₃ incorporated into
96 CTMs (Massad et al., 2010). Based on published data on χ_s in relation to different plant
97 species, growth stages, N supply etc., Massad et al. (2010) derived a new operational
98 parameterization for integrating bi-directional NH₃ exchange into CTMs, However,
99 uncertainties still exist for its parameterization, partially due to the following two
100 drawbacks: 1) measurement of χ_s for different ecosystems, specific to forests, is very
101 sparse and is only considered for a single growth stage of plants; 2) the relationships
102 established between N fertilizer application and χ_s remain uncertain due to a lack of co-
103 measurement of χ_s with different organic fertilizer (manure, slurry and urea) application
104 rates. In addition, the actual parameterization of NH₃ exchange models requires large
105 databases accounting for the variability of χ_s . To our knowledge, there is only one
106 process-based model developed by Riedo et al. (2002) for grasslands which accounts
107 for the plants N nutrition and growth stage in calculating χ_s . However, as χ_s is not only
108 driven by N input to the ecosystem and plant growth stage, it may be a strongly
109 regulated process that depends on environmental changes such as elevated ground-level

110 O₃.

111 Ground-level O₃ can be considered as the most phytotoxic air pollutant due to
112 visible injury to a variety of plants and the rising concentrations in different regions of
113 the world (Cooper et al., 2014; Feng et al., 2014). It affects photosynthetic parameters
114 (e.g., stomatal conductance (g_s), light-saturated CO₂ assimilation rate (A_{sat}),
115 intercellular CO₂ concentration (C_i) and chlorophyll (Chl) content) of forest species to
116 a varying extent (Li et al., 2017). In contrast, atmospheric N deposition represents an
117 important nutrient from the environment for plants (Liu et al., 2010). In N-limited
118 ecosystems (e.g., forest) N deposition might enhance photosynthetic activity (i.e.
119 photosynthetic enzyme activity) and net primary productivity (N fertilization effect)
120 (Liu et al., 2011). In the context of an N-saturation ecosystem, however, N deposition
121 may render plants more susceptible to pollutants and natural environmental stressors
122 (Cardoso-Vilhena and Barnes, 2001). Ozone and N induced changes in the growth and
123 metabolism of plants may affect the χ_s of plants due to a clear link between χ_s and
124 photosynthetic parameters. For example, Mattsone and Schjoerring (1996) showed
125 that leaf NH₃ emission from *Hordeum vulgare L. cv. Golf* plants showed a consistent
126 diurnal pattern with photosynthesis but the opposite trend with g_s . Furthermore,
127 Schjoerring et al. (1998) found that NH₃ emission from leaves of *Brassica napus L.*
128 plants increased with Chl degradation. Such results demonstrate that there are
129 corresponding influences of those parameters on χ_s , which positively impacts leaf NH₃
130 emission (Massad et al., 2010). In this context, understanding the effects of elevated O₃
131 and N as well as their influence on the plant physiological parameters controlling χ_s is
132 important for prediction of χ_s . Unfortunately, the relevant information for different
133 forest species is still unknown, significantly restricting the optimization of the χ_s
134 parameter in CTM models.

135 Poplars are widespread deciduous plants in temperate and boreal forests. In China,
136 poplar is a native species, with a cultivated area of more than 10 million ha (Yuan et al.,
137 2016). We designed an experiment to investigate for the first time the individual effects
138 of elevated N deposition (with controlled application of urea) and O₃ and their
139 interactions on χ_s of hybrid poplar clone '546' (*Populus deltoides cv. 55/56 x P. deltoides*

140 *cv. Imperial*). In addition, we estimated the relationships between photosynthetic
141 parameters (g_s , A_{sat} , C_i and Chl) and χ_s , and discuss how N and O₃, as well as their-
142 driven modifications in the aforementioned photosynthetic parameters, respectively
143 affect χ_s .

144 **2. Materials and methods**

145 *2.1. Experimental site and plant materials*

146 The study was conducted in Yanqing Field and Experimental Basin, Tangjiapu
147 village, Yanqing District (40°29'N, 115°59'E, 500 m.a.s.l.), about 74 km northwest of
148 Beijing city centre. When the winds come from the north or northwest, this basin is
149 located upwind of the Beijing urban area. The site is characterized by a continental
150 monsoon climate, with mean annual temperature of 9 °C and mean annual precipitation
151 of 400-500 mm.

152 Rooted cuttings of hybrid poplar clone '546' (*Populusdeltoides cv. 55/56 x P.*
153 *deltoides cv. Imperial*) were planted on 7 May 2017 and cultivated in individual 20 L
154 circular plastic pots when they were about 31 days old. The plots were filled with local
155 light loamy farmland soil, which was excavated at 0-10 cm depth, sieved out by a 0.3
156 mm pore mesh and then thoroughly mixed for homogeneity. Plants with similar height
157 (ca. 27.2 cm) and basal stem diameter (ca. 4.5 mm) were selected and pre-adapted to
158 open-top chambers (OTCs, octagonal base, 12.5 m² of growth space and 3.0 m height,
159 covered with toughened glass) for 10 days before O₃ fumigation. All seedlings were
160 manually irrigated at 1-2 day intervals in order to keep moisture at a similar level to
161 that in farm fields.

162 *2.2. O₃ and N treatments*

163 The experiment was conducted in six OTCs with two O₃ treatments: charcoal-
164 filtered ambient air (CF), and elevated O₃ (E-O₃, non-filtered air with targeted O₃
165 addition of 40 ppb during fumigation). Each treatment had three OTC replicates, and
166 six potted plants were randomly distributed in each OTC. The O₃ fumigation was
167 performed from 10 June to 22 September 2017. The daily fumigation time was 10 h
168 (from 08:00 till 18:00), except on rainy days. During the fumigation period, the

169 averaged O₃ concentrations in CF and E-O₃ were 24.0 and 80.6 ppb, respectively, and
170 AOT40 (accumulated hourly O₃ concentration above a threshold of 40 ppb) was 2.4
171 and 41.6 ppm h, respectively. Ozone was generated from pure oxygen using an
172 electrical discharge O₃ generator (HY003, Chuangcheng Co., Jinan, China) and mixed
173 with ambient air using a fan. Ozone concentrations inside the OTCs were continuously
174 monitored at approximately 10 cm above the plant canopy using two ultraviolet (UV)
175 absorption O₃ analyzers (Model 49i-Thermo, Thermo Scientific, Massachusetts, USA,
176 one for three OTCs). The analyzers were calibrated with a 49iPS calibrator (Thermo
177 Scientific) before the experiment and once a month during the experiment.

178 In addition to the O₃ treatments, two N treatments were applied with three
179 replicates: control (N0, no N added), and moderate N, (N50, 50 kg N ha⁻¹ yr⁻¹). For N50,
180 N additions were applied five times (13 June, 29 June, 16 July, 1 August, 17 August) to
181 the soil with dilute urea solutions by using a 50 mL plastic bottle and the control pots
182 received equal amounts of pure water. In total, N50 received 0.245 g N per pot (i.e.
183 0.526 g urea per pot) throughout the experiment. This application rate (0.245 g N per
184 pot) can be projected to a dose of 50 kg N ha⁻¹ based on the area (0.049 m²) of each pot.
185 The concentrations of NH₄⁺-N and NO₃⁻-N in the soil of N0 treatment were 6.5 ± 2.2
186 and 4.6 ± 1.4 mg N kg⁻¹ wet soil, respectively (unpublished data).

187 2.3. *Measurements of physiological parameters*

188 Measurements of gas exchange, leaf temperature and chlorophyll content were
189 performed during two periods, i.e., at the end of July and August, 2017 (on 30 and 31
190 July, and on 29 and 31 August, respectively). For all plants, middle leaves were selected
191 as targeted leaves, which were 11th to 13th fully expanded leaves from the apex and
192 comprised the main part of the leaves on each plant. A portable photosynthetic system
193 fitting with a 6400-40 leaf chamber fluorometer (LI-6400-40, LI-COR Co., USA) was
194 used to measure gas exchange and leaf temperature from one middle leaf between 9:00
195 and 11:00 h. For the measurements, the photosynthetic photon flux density was set at
196 1200 μmol m⁻² s⁻¹, the CO₂ concentration of air entering the leaf at 400 μmol mol⁻¹ and
197 the relative humidity at 50-60%. The measured parameters were A_{sat} , g_s , and C_i . It

198 should be noted that the 2-h measurement duration has only a small influence on g_s ,
199 since the influencing factors on g_s (e.g., leaf temperature, vapor pressure deficit,
200 ambient CO₂ concentration, Hu et al., 2015) have a small fluctuation during the
201 corresponding time period (data not shown), and the photosynthetic photon flux density
202 leaf was fixed. During the entire experimental period, a total of 72 leaf samples were
203 measured.

204 Immediately after measurements of gas exchange and leaf temperature, two leaf
205 discs were sampled from the targeted leaf and then extracted with 2 mL 95% ethanol
206 solution in the dark for at least 72 h at 4 °C. The Chl content in the extract was
207 determined using the specific absorption coefficients (Lichtenthaler, 1987).

208 2.4. Determination of apoplastic NH₄⁺ and H⁺ concentration

209 A slightly modified version of the vacuum infiltration technique developed by
210 Husted and Schjoerring (1995) was employed to determine apoplastic NH₄⁺ and H⁺
211 concentrations. Immediately after measurements of physiological parameters, the
212 targeted leaf was cut and washed with high-purity water (18.2 Ω), in order to avoid any
213 contamination from air pollutants (e.g., particulate NH₄⁺). The leaf was then blotted dry
214 with clean absorbent paper towel and the central petiole was removed. The leaves were
215 separated into three replicates and then weighted, infiltrated with 280 mM sorbitol
216 solution using a 60 mL plastic syringe with a series of vacuum/pressure for 5 min. The
217 vacuum/pressure process was automatically applied with an intercellular fluid extractor
218 (NS-AFE-1, Pulanta Co. Suzhou, China). The infiltrated leaves were quickly rinsed
219 with high-purity water, blotted dry and re-weighted. The leaves were then rolled,
220 inserted into tubes and centrifuged at 9000 r min⁻¹ for 10 min at 4°C to collect the
221 apoplastic solution. Cytoplasmic contamination of the apoplast during the extraction
222 procedure was checked by performing the extraction using a buffered solution (0.1 M
223 Ntris[hydroxymethyl]methyl-2-aminoethanesulphonic acid, 2 mM dithiothreitol and
224 0.2 mM EDTA), and comparing the activity of Malate Dehydrogenase (MDH) in the
225 apoplastic extracts to its activity in bulk tissue extracts as described by Husted and
226 Schjoerring (1995). The contamination was less than $1.2 \pm 1.1\%$ of MDH activity in

227 apoplast extract relative to bulk tissue extract. The extracted solution was then frozen
228 and stored at -20 °C prior to chemical analysis.

229 The NH_4^+ concentrations in the apoplastic extracts were measured with an AA3
230 continuous-flow analyzer (BranCLuebbe GmbH, Norderstedt, Germany). The
231 detection limit of NH_4^+ was 0.01 mg N L^{-1} . The pH of the extracted solution was
232 measured with an InLab micro electrode (Mettler Toledo, Udorf, Switzerland). The
233 dilution of the apoplastic solution was determined spectrophotometrically at
234 wavelength 492 nm for the sorbitol, which allowed the calculation of a dilution factor
235 (Hove et al., 2002). The concentration of apoplastic NH_4^+ and H^+ was corrected for
236 dilution during the extraction procedure by multiplication with the dilution factor (F_{dil}).

237 The aqueous volume of the apoplast (V_{apo} , mL g^{-1} leaf fresh weight (LFW)) was
238 estimated using the equation (Hove et al., 2002):

$$239 \quad V_{\text{apo}} = \frac{V_i(F_{\text{d,sorb}}-1)}{\text{LFW}} \quad (1)$$

240 where V_i is the infiltration volume which was calculated by assuming a leaf density
241 of 1 g cm^{-3} the difference in weight before and after infiltration, $F_{\text{d,sorb}}$ is the dilution
242 factor of sorbitol.

$$243 \quad F_{\text{dil}} = \frac{V_{\text{apo}}+V_{\text{air}}}{V_{\text{apo}}} \quad (2)$$

244 where V_{air} is the air volume inside the leaf ($\text{cm}^3 \text{g}^{-1}$ LFW) which was measured by
245 infiltrating leaves with low-viscosity silicone oil (10 mPa s). Based on the increase in
246 weight and oil density (0.93 g cm^{-3}), the V_{air} was estimated to be approximately 0.16
247 mL g^{-1} throughout the experiment.

248 2.5. Determination of the leaf tissue NH_4^+ concentration

249 The leaf segments were cut into small pieces, frozen in a ceramic mortar with
250 liquid N (-210 °C), and quickly ground into a homogenous powder using a ceramic
251 pestle. The weighed samples (approximately 1.0 g per sample) were put into a 5 mL
252 centrifuge tube with 4 mL of high-purity water, followed by centrifugation at 2000 g
253 (4°C) for 10 min (Loubet et al., 2002). The supernatant was then decanted and filtered
254 through a syringe filter (0.45 μm , Tengda Inc., Tianjin, China) to remove large plant

255 tissues. The filtered solution was frozen and stored at -20 °C until analysis for NH₄⁺
256 using an AA3 continuous-flow analyzer as mentioned before.

257 2.6. Calculation of NH₃ stomatal compensation point

258 The stomatal compensation points were derived using the apoplast pH and NH₄⁺
259 concentrations (Loubet et al., 2002) according to the equation:

$$260 \quad \chi_s = M_{\text{NH}_3} \times K_H \times K_D \times \frac{[\text{NH}_4^+]}{[\text{H}^+]} \times 10^9 \quad (3)$$

261 where χ_s is the stomatal compensation point in $\mu\text{g NH}_3 \text{ m}^{-3}$, M_{NH_3} is the molecular
262 mass of NH₃ in g mol^{-1} , The ratio of apoplast NH₄⁺ to apoplast H⁺ concentration, called
263 the emission potential (expressed as Γ_s), is temperature independent and dimensionless
264 (Massad et al., 2010). K_H is the Henry constant and K_D is the dissociation constant. The
265 product $K_H K_D$ depends on temperature and was calculated following the method of
266 (Hill et al., 2001):

$$267 \quad K_H K_D = \frac{161512}{T_{\text{leaf}}} \times 10^{\frac{-4507.11}{T_{\text{leaf}}}} \quad (4)$$

268 where T_{leaf} is leaf temperature in Kelvin.

269 2.7. Statistical analysis

270 Data of each investigated variable from three plants per OTC were averaged and
271 then used as the statistical unit (N=3). Prior to analysis, all data were tested for
272 normality using the Shapiro-Wilk's W-test and for homogeneity of variance using
273 Levene's-test to determine whether data should be transformed to satisfy statistical
274 assumptions. A split-plot design was used, with O₃ as the main plot, N level as sub-plot
275 and measurement dates as repeat-measurement. A repeated measure analysis of
276 variance (ANOVA) with a mixed linear model was then conducted to examine the
277 effects of O₃, N, measurement dates and their interactions on physiological parameters
278 and χ_s as well as other parameters. Tukey's Honestly Significant Difference (HSD) test
279 was applied to examine the significant differences. Analysis of covariance (ANCOVA)
280 was performed to test the significance of difference in the slopes of the linear
281 relationship between χ_s and physiological parameters. All statistical analyses were
282 performed in R version 3.3.3 (<http://www.r-project.org/>), with significant level set at

283 $P < 0.05$. All the data were shown as mean \pm standard deviation (SD) of three OTC
284 replicates.

285 3. Results

286 For all investigated variables, similar and non-significant responses to E-O₃ and
287 N50 were found between the two measurement dates, i.e., July and August (**Figs. 1 and**
288 **2**). Based on integrated analysis of all data from all N and O₃ treatments and the two
289 measurement dates, the main results are presented below.

290 3.1. Photosynthetic parameters

291 For all investigated variables (A_{sat} , g_s , C_i and Chl), the interactions of O₃ and N
292 were not significant, but the individual effects of them were significant for most
293 variables (**Table 1**). Relative to CF, E-O₃ significantly reduced A_{sat} by 55%, whereas
294 A_{sat} has a small non-significant increase (6%) in NF50 relative to N0 (**Fig. 1a, Table 1**).
295 A_{sat} significantly decreased (by 24%) in August relative to that in July, when averaged
296 across all treatments. The effects of N and O₃ on g_s were both not significant, whereas
297 measurement date significantly affected g_s (**Fig. 1b, Table 1**). Similar to A_{sat} , g_s
298 significantly decreased by 30% in August compared with that in July.

299 Ozone significantly influenced C_i and Chl, whereas N had no significant effects
300 on them (**Fig. 1c d, Table 1**). C_i was significantly increased by E-O₃ (+7%) compared
301 with CF, and also was significantly higher (6%) in August than in July. Conversely, Chl
302 was significantly reduced by E-O₃ (-30%), and significantly decreased (by 57%) in
303 August.

304 3.2. Leaf apoplastic NH_4^+ and pH, and leaf tissue NH_4^+

305 **Fig. 2a-c** shows the responses of leaf apoplastic NH_4^+ concentration and pH, and
306 leaf tissue NH_4^+ concentration to E-O₃ and N50. The interactions between O₃ and N
307 and/or measurement dates were not significant for all those three variables (**Table 1**).
308 However, individual effects of them on apoplastic NH_4^+ concentrations and pH all
309 reached statistically significant levels. Similarly, leaf tissue NH_4^+ concentration was
310 significantly influenced by both O₃ and measurement dates, but not by N.

311 Averaged apoplastic NH_4^+ concentration was significantly reduced (by 15%) in E-

312 O₃ plants compared with CF plants (**Fig. 2a, Table 1**). By contrast, the mean
313 concentration was significantly increased (by 27%) in N50 plants compared with that
314 in N0 plants. A significant increase (14%) of the mean occurred in August relative to
315 July. As for apoplastic pH, two small but significant reductions (both 4%) of the mean
316 were found in E-O₃ and N50 plants compared with those in CF and N50 plants,
317 respectively (**Fig. 2c, Table 1**). Also, the mean pH was significantly lower (15%) in
318 plants grown in August than in July.

319 In contrast to apoplastic NH₄⁺, the mean tissue NH₄⁺ concentration significantly
320 increased (by 15%) in E-O₃ plants relative to that in CF plants, whereas a small and
321 non-significant difference in the mean was found between N0 and N50 plants (**Fig. 2b,**
322 **Table 1**). The mean concentrations decreased significantly (on average by 6%) in
323 August relative to July.

324 3.3. Emission potential (Γ_s) and stomatal compensation point (χ_s)

325 As presented in **Table 1**, both O₃ and measurement dates significantly affected Γ_s ,
326 whereas N had no significant effect on it. Also, no significant interactions between O₃,
327 N and/or measurement dates were observed. E-O₃ treatment relative to CF significantly
328 reduced Γ_s by 39% (**Fig. 2d**). Γ_s was significantly reduced (by 85%) in August
329 compared with that in July.

330 χ_s was significantly lower in E-O₃ than in CF (0.29 ± 0.29 and $0.48 \pm 0.45 \mu\text{g NH}_3$
331 m^{-3}), and also in N50 than N0 (0.34 ± 0.36 and $0.42 \pm 0.41 \mu\text{g NH}_3 \text{m}^{-3}$) (**Fig. 3, Table**
332 **1**). A significant interaction of O₃ and N was found (**Table 1**). χ_s was significantly lower
333 in August than in July (0.07 ± 0.05 and $0.70 \pm 0.29 \mu\text{g NH}_3 \text{m}^{-3}$) (**Fig. 3, Table 1**).

334 3.4. Correlations between stomatal compensation point (χ_s) and photosynthetic 335 parameters

336 χ_s was positively and significantly correlated with A_{sat} and g_s (**Fig. 4a, b**), whereas
337 a negative and significant correlation between χ_s and C_i was observed (**Fig. 4c**). The
338 correlation between χ_s and Chl was positive and significant in July, but was not
339 significant in August (**Fig. 4d**).

340 4. Discussion

341 4.1. Effect of N application

342 The application rate of urea fertilizer in the present experiment ($50 \text{ kg N ha}^{-1} \text{ yr}^{-1}$)
343 is approximately 2.3 and 3 times higher than the averages of N deposition over China
344 ($16 \text{ kg N ha}^{-1} \text{ yr}^{-1}$ in 2008-2012 period, [Zhao et al., 2017](#)) and in China's forests (22 kg
345 $\text{N ha}^{-1} \text{ yr}^{-1}$ in 1995-2010 period, [Du et al., 2014](#)), respectively. It is also approximately
346 1.7-5.0 times greater than reported values during recent years in the N deposition
347 hotspots of western Europe (20.0 to $28.1 \text{ kg N ha}^{-1} \text{ yr}^{-1}$, [Vet et al., 2014](#)), and North
348 America (10.0 to $20.0 \text{ kg N ha}^{-1} \text{ yr}^{-1}$, [Li et al., 2016](#)). According to [Liu et al. \(2013\)](#), N
349 deposition increased by approximately $8 \text{ kg N ha}^{-1} \text{ yr}^{-1}$ between the 1980s and the 2000s
350 in China. Also, total N deposition is expected to have a 5-10% increase in the year 2050
351 relative to 2005 ([Kanakidou et al., 2016](#)). In view of the above, the level of N addition
352 in this study is sufficient to assess the ecological effects of enhanced N deposition
353 expected in the future. However, it should be pointed out that application of N to the
354 soil is not able to fairly reflect the process of N deposition in the real-world, in which
355 natural deposited N would at least partially be captured by the canopy. As reported by
356 [Du et al. \(2014\)](#), for example, canopy captured dry deposition of total inorganic N in
357 China's forest was estimated at $6.9 \text{ kg N ha}^{-1} \text{ yr}^{-1}$.

358 Apoplastic NH_4^+ concentration is one of the key factors in controlling χ_s , which is
359 associated with the status of leaf N and external N supply (e.g., N fertilization and
360 atmospheric deposition) ([Herrmann et al., 2009](#); [Massad et al., 2008](#)). The apoplastic
361 NH_4^+ concentrations measured for the N0 and N50 treatments (but without E-O₃) were
362 0.10 ± 0.01 and $0.13 \pm 0.01 \text{ mM}$, respectively (**Fig. 2a**). To our knowledge published
363 data on apoplastic NH_4^+ concentrations in leaves of poplar clone 546 is unavailable,
364 making a direct comparison with other studies impossible. However, our measured
365 value for N0 treatments were close to that reported for *Fagus sylvatica* growing in July
366 and August (0.11 mM , [Wang et al., 2011](#)). Compared with agricultural crops, our
367 measured value for N0 treatments was higher than that reported for barley (0.04 mM ,
368 [Mattsson et al., 1998](#)), and was close to the value of 0.10 measured for oilseed rape
369 ([Massad et al., 2009](#)) both growing on N0. The value for plants grown on N50 was
370 similar to that measured for oilseed rape (0.18 mM with 6 mM NO_3^- , [Schjoerring et al.,](#)
371 [2002](#)), and was lower than the value of 1.9 mM observed for barley grown on 5 mM

372 NH_4^+ (Mattsson et al., 1998). As expected, enhanced N input (N50) significantly
373 increased the apoplastic NH_4^+ concentration (**Fig. 2, Table 1**), probably due to increased
374 soil N availability. This result is similar to the findings of Massad et al. (2009) that the
375 NH_4^+ concentrations in leaf apoplast of oilseed rape increased significantly with rising
376 N treatments (aside from NO_3^- supply).

377 Besides apoplastic NH_4^+ concentration, the pH of the apoplast may be the most
378 important factor determining χ_s . There is evidence that NH_4^+ -fed plants have reduced
379 apoplastic pH compared to NO_3^- -fed plants, e.g., sunflower (Hoffmann et al., 1992),
380 soybean (Kosegarten and Englisch, 1994) and barley (Mattsson et al., 1998), probably
381 due to a root rather than shoot assimilation of N (Pearson et al., 1998). Application of
382 urea fertilizer in the present experiment probably enhanced soil NH_4^+ level via urea
383 hydrolysis, which further significantly increased apoplastic NH_4^+ concentrations (**Fig.**
384 **2a**) via root assimilation and the subsequent transport of NH_4^+ to the foliar apoplast in
385 the xylem (Mattson et al., 1998). This behaviour, along with NH_4^+ uptake-induced
386 acidification may offer an explanation for lower apoplastic pH (ranging from 4.6 to 6.0,
387 **Fig. 2c**) of poplar 546 compared with those reported for most plant species (between
388 5.0 and 6.5, Grignon and Sentenac, 1991). However, it is still a little controversial how
389 the type on mineral N supply (NO_3^- versus NH_4^+) affects apoplastic pH in leaves.
390 Nitrate type mineral N (NO_3^-) has been shown to an alkalization while NH_4^+ induced
391 an acidification (Hoffmann et al., 1992; Mengel et al., 1994). Sattelmacher. (2001)
392 suggested that nitrate effectively leads to higher pH levels but only depending on its
393 concentration in the xylem sap. However, NH_4^+ nutrition didn't show any effect on leaf
394 apoplast pH at low concentrations. Finnemann and Schjoerring (1999) questioned this
395 result and show a relation between root N supply type and NH_4^+ concentrations in the
396 xylem sap and in the leaf apoplast. They explain this result by high levels of
397 photorespiration (Kronzucker et al., 1998; Nielsen and Schjoerring, 1998). However
398 there is a clear effect on apoplastic pH due to foliar application of NH_4^+ which leads to
399 lowed pH values (Peuke et al., 1998). On the other hand, fumigation with
400 NH_3 decreases H^+ activity (Hanstein et al., 1999).

401 Enhanced N input significantly increased both apoplastic NH_4^+ and H^+

402 concentration with a similar significant level (**Figs. 2a,c and Table 1**). Conversely, χ_s
403 was significantly reduced (by 19%) by N50 (**Fig. 3**). These results, together with the
404 relatively low calculated χ_s throughout, especially in August (**Fig. 3**), suggest that χ_s
405 appears to be pH-driven in this study. The apoplastic pH of *Phaseolus vulgaris* has been
406 found to become alkalized during photosynthesis ([Raven and Farquhar, 1989](#)).
407 Similarly, we found that the N load marginally significantly ($P=0.057$) increased A_{sat} of
408 poplar 546 (**Fig. 1a, Table 1**), which significantly positively correlated with apoplastic
409 pH (**Fig. 5a**) but had no significant relationship with apoplastic NH_4^+ concentration
410 ($R^2=0.09$, $P=0.141$). These results provide an explanation for a significant and positive
411 relationship observed between A_{sat} and χ_s (**Fig. 4a**). Although such an increase in
412 apoplastic pH occurred due to non-significant increased A_{sat} by N load, it is insufficient
413 to offset NH_4^+ uptake-induced apoplast acidification, leading to relatively low χ_s .

414 4.2. Effect of O_3 application

415 According to monitoring results for the 2014-2016 period in 187 Chinese cities,
416 the mean daily 8-h O_3 concentrations peak in summer reached up to 114.30 ± 23.78 ppb
417 ([Li et al., 2017](#)). Obviously, the O_3 level in E- O_3 was within the range of current O_3
418 levels in China and was also in the range of future expected concentrations in warm and
419 sunny areas of the world at the end of this century ([The Royal Society 2008](#); [IPCC](#)
420 [2013](#)). The dose of O_3 (41.6 ppm h in AOT40) in E- O_3 by far exceeded the O_3 exposure
421 limit of 5 ppm h accumulated over the growing season for forest protection ([CLRTAP,](#)
422 [2015](#)) and 12 ppm h for poplar protection ([Hu et al., 2015](#)). As anticipated, O_3 -induced
423 injuries to poplar 546 were detected in E- O_3 despite N fertilization (e.g., reduction of
424 A_{sat} and Chl, **Fig. 1a, d**), thus confirming that poplar 546 is a very sensitive species to
425 O_3 ([Shang et al., 2017](#)).

426 E- O_3 significantly increased C_i and decreased A_{sat} and Chl, respectively, but did
427 not significantly affect g_s (**Figs. 1 and Table 1**). These results are consistent with the
428 findings of [Shang et al. \(2017\)](#) for polar clone 546. Similarly, a previous study showed
429 that O_3 can substantially reduce A_{sat} in most plants, and also detected an uncoupled
430 relationships between A_{sat} and g_s ([Zhang et al., 2012](#)). This can be explained by the fact
431 that the O_3 -induced reduction in A_{sat} is largely ascribed to non-stomatal factors, i.e.

432 impaired physiological activity of mesophyll cells (Akhtar et al., 2010; Feng et al.,
433 2016). Although each investigated photosynthetic parameter was significantly
434 influenced by O₃, interactions of O₃ and N were not significant (Table 1). This is similar
435 to the findings of Harmens et al. (2017) that no any interactions between O₃ and N
436 regarding photosynthetic parameters, chlorophyll content, g_s, N content in senesced
437 leaves and leaf number for *Betula pendula* saplings.

438 We found that E-O₃ significantly reduced the calculated χ_s (Fig. 3). This is most
439 likely related to a decline in apoplastic pH resulting from O₃-induced changes in
440 photosynthetic parameters, i.e., decreased A_{sat} and Chl, and increased C_i (Fig. 1a,c,d,
441 Table 1). This is because in addition to A_{sat} , both Chl and C_i correlated significantly
442 with χ_s and apoplastic pH (Figs. 4c,d and 5b,c). In addition, there was a large positive
443 response of ammonia emission (from young barely) to photosynthesis (Mattsson and
444 Schjoerring, 1996), mainly due to the fact that NH₃ assimilation by plants requires
445 carbon skeletons generated from photosynthesized carbohydrates for the synthesis of
446 amino acids (Huppe and Turpin, 1994). In this regard, a significant reduction in A_{sat} can
447 also give rise to declines in apoplastic NH₄⁺ concentration. Similar to N, ozone has a
448 greater impact on apoplastic pH than on apoplastic NH₄⁺ concentration, as
449 demonstrated by the significant reduction of Γ_s by O₃ (Fig. 2d, Table 1); this therefore
450 led to a significant reduction in χ_s (Fig. 3, Table 1).

451 4.3. Combined effects of N and O₃ application

452 The present results showed that N and O₃ interacted significantly in χ_s (Table 1).
453 Further analysis showed that χ_s in N0*E-O₃ ($0.28 \pm 0.30 \mu\text{g NH}_3 \text{ m}^{-3}$) was 50% lower
454 than that in N0*CF ($0.56 \pm 0.49 \mu\text{g NH}_3 \text{ m}^{-3}$), suggesting a negative effect of E-O₃ on
455 χ_s . This, together with a 28% decrease in χ_s when comparing χ_s in N50*E-O₃ ($0.29 \pm$
456 $0.31 \mu\text{g NH}_3 \text{ m}^{-3}$) with that in N50*CF ($0.40 \pm 0.44 \mu\text{g NH}_3 \text{ m}^{-3}$), also indicate that N
457 application can mitigate the negative effects of O₃ on χ_s .

458 Our selected poplar 546 belongs to deciduous broadleaf species. To make a
459 preliminary assessment of whether Chinese deciduous broadleaf forests (Fig. 6a) act as
460 a source or a sink for atmospheric NH₃, we compared the calculated χ_s with mean
461 atmospheric NH₃ concentration in July (Fig. 6b) and August (Fig. 6c) during 2008-

462 2012 period. The concentrations were modeled using the GEOS-Chem model and fitted
463 with the surface NH₃ measurements, see details in [Zhao et al. \(2017\)](#)). The results of
464 the comparison show that the modeled NH₃ concentrations over approximately 91%
465 and 100% of total land area exceeded the calculated χ_s for elevated N and O₃ treatment
466 in July (average 0.54 $\mu\text{g NH}_3 \text{ m}^{-3}$) and August (average 0.03 $\mu\text{g NH}_3 \text{ m}^{-3}$), respectively.
467 It should be noted that such percentages are considered to be approximate estimates, as
468 χ_s may vary among different forest species, and the current atmospheric NH₃
469 concentration cannot represent future NH₃ levels. Nevertheless, we may conclude that
470 under the current ambient NH₃ concentrations in China the canopy of deciduous
471 broadleaf forests is unlikely to be a major source of NH₃ emission during summertime.

472

473 *4.4. Dependence on measurement date*

474 χ_s can be influenced by plant developmental stage since leaf apoplastic NH₄⁺
475 concentration and pH varies among leaves of different ages ([Hill et al., 2002](#)). [Mattsson
476 and Schjoerring \(2003\)](#) reported that, for ryegrass (*Lolium perenne*), both apoplastic
477 and tissue NH₄⁺ concentrations were 2-3 times higher in senescing or injured leaves
478 (with visual symptoms of senescence) compared with green leaves. The present study
479 shows that leaf apoplastic NH₄⁺ concentrations significantly increased in August
480 compared with those in July, whereas a significant reduction was found for leaf tissue
481 NH₄⁺ concentration (**Fig. 2a, b**). In addition, a negative relationship was observed
482 between NH₄⁺ concentrations in apoplast and in tissue (**Fig. 5d**). These results together
483 indicated that NH₄⁺ is actively transported from the leaf tissue to the apoplast. This
484 explanation is supported by evidences from earlier studies showing that apoplastic fluid
485 in leaves constitutes a highly dynamic NH₄⁺ pool, to which NH₄⁺ is constantly supplied
486 via NH₃ efflux from the mesophyll cells ([Nielsen and Schjoerring, 1998](#); [Schjoerring et
487 al. 2000](#)).

488 Regarding apoplastic pH, the values measured in August were significantly
489 reduced compared to July, and almost all were <5 (**Fig. 2c, Table 1**), for which an
490 explanation is the combined effect of NH₄⁺ uptake-induced acidification (see Sect. 4.1)
491 and O₃-accelerated leaf senescence ([Gao et al., 2017](#)). As reported by [Mattsson and](#)

492 [Schjoerring \(2003\)](#), leaf aging from green leaves to yellow tips resulted in a pronounced
493 decrease of pH by more than 1 unit. Thus, a significantly lower A_{sat} in August resulting
494 from accelerated leaf senescence (**Fig. 1a, Table 1**) also contributed to lower apoplastic
495 pH due to the existence of apoplast alkalinization during photosynthesis as mentioned
496 earlier.

497 χ_s was significantly reduced in August compared with July (**Fig. 3**). This is likely
498 due to the greater impact of measurement date on apoplastic pH than on apoplastic
499 NH_4^+ concentration as indicated by their respective significant level (**Table 1**). The
500 change in stomatal opening is an important control mechanism for the regulation of
501 influxes and outfluxes of NH_3 into or out of the leaves because the conductance for
502 diffusion of NH_3 is affected ([Schjoerring et al., 1998](#)). We found that g_s significantly
503 decreased in August (**Fig. 1b, Table 1**). Also, a positive and significant relationship was
504 observed between g_s and χ_s (**Fig. 4b**); this is mainly caused by measurement date as
505 both E- O_3 and N did not significantly affect g_s . These results together suggested that a
506 significant reduction of g_s also contributed to a reduction in χ_s .

507 *4.5. Uncertainty and recommendations*

508 In the present study, χ_s is calculated based on direct measurements of leaf
509 apoplastic NH_4^+ concentration and pH by means of extraction of the apoplastic fluid
510 with successive vacuum infiltration/centrifugation technique ([Husted and Schjørring.,](#)
511 [1995](#)). Although this technique has been successfully applied to several plant species in
512 the field ([Herrmann et al., 2009](#); [Mattsson et al., 2009](#)), it is subject to uncertainties
513 regarding potential regulation of apoplastic NH_4^+ concentration and pH by the plant
514 during the infiltration and buffering effects ([Massad et al., 2009](#)). For example, [Nielsen](#)
515 [and Schjørring \(1998\)](#) showed that apoplastic NH_4^+ concentration in *Brassica napus* L.
516 appeared to be regulated during infiltration. However, [Hill et al. \(2001\)](#) did not detect
517 such a homeostasis for apoplastic NH_4^+ concentration in *Luzula sylvatica* (Huds.) Gaud.
518 Following the method of [van Hove et al. \(2002\)](#), F_{dil} , calculated based on determination
519 of V_{air} and V_{apo} (**Equ. 2**), was applied to correct apoplastic concentrations. V_{apo} values
520 obtained in the present work varied from 0.06 to 0.23. These values fit well into the
521 range found by other researchers for different plant species ([Van Han et al., 2001, 2002](#)).

522 The measured V_{air} ($0.16 \text{ ml g}^{-1} \text{ LFW}$) was also comparable to values ($0.21 \text{ mL g}^{-1} \text{ LFW}$)
523 reported for *Lolium perenne* L. (Van Han et al., 2002). These results indicate that the
524 value for F_{dil} determined in the present study was acceptable. However, due to a lack of
525 information regarding infiltration of poplar 546, use of F_{dil} might also result in some
526 uncertainties in apoplastic NH_4^+ concentrations and pH, and probably in χ_s if there is a
527 potential difference in the buffering capacity between them.

528 The vacuum infiltration/centrifugation method is also subject to some uncertainty
529 due to the strong possibility of cytoplasmic contamination of the apoplast during the
530 extraction procedure (Lohaus et al., 2001). We estimated the error in this method by
531 assaying the contamination of the apoplast by MDH activity. The cytoplasmic
532 contamination in the present work was about 1.2%.

533 χ_s obtained in the current study was calculated at the leaf scale and only for the
534 middle leaf position. However, χ_s may differ significantly depending on leaf position
535 (e.g., upper, middle and lower) due to difference in the N status of the leaves. Thus, the
536 resulting effects of enhanced N and O_3 on χ_s are not enough to represent the
537 characteristics of the entire-plant. Furthermore, the present experiment was designed
538 based on OTC chambers. However, OTCs have effects of their own, such as differences
539 in microclimate (e.g., air temperature and humidity), fixed gas flow and limited space,
540 which could over-estimate or under-estimate the effects of O_3 on plants (Feng et al.,
541 2010). Note that χ_s is shown to be influenced by air temperature, partly by affecting the
542 amount of NH_3 dissolved in the apoplast, and partly by affecting the leaf tissue NH_4^+
543 generation (or assimilation)-associated physiological processes (Schjoerring et al.
544 1998). To more accurately assess the effects of N, O_3 and/or plant growth stage on χ_s ,
545 at least the two following developments are recommended in future work: 1) to employ
546 open-air fumigations (O_3 -FACE systems, Paoletti et al., 2016), and 2) to investigate
547 vertical profile of χ_s at plant scale

548 4.6. Conclusions and Implications

549 In summary, the current study is the first time to investigate the combined effects
550 of O_3 exposure and use of urea as N load on χ_s of forest species (i.e., poplar clone 546).
551 Our results demonstrated that elevated O_3 significant reduced χ_s , in tandem with A_{sat} ,

552 Ci and Chl. Also, urea addition significantly reduced χ_s , and can mitigate the negative
553 effects of O₃ on χ_s (**Fig. 3, Table 1**). Our findings filled knowledge gaps in the influence
554 of O₃ on χ_s , and provided valuable and additional information on effect of N addition
555 on χ_s , which is commonly expected to increase considerably with input of the different
556 types of inorganic N fertilizer applied (Massad et al., 2010). In addition, we
557 demonstrated a significant reduction of χ_s in the context of O₃-accelerated senescence,
558 in contrast to the common view that χ_s is affected by the plant's development stage
559 and may peak at senescence (Hill et al., 2002; Mattsson and Schjoerring, 2003).
560 Based on these findings, we propose that current parameterizations of χ_s in chemical
561 transport models should be optimized to partially respond to changes in environmental
562 conditions (e.g., elevated N and/or O₃). In addition, A_{sat} , g_s and Chl significantly and
563 positively corrected with χ_s , whereas a significant and negative relationship was
564 observed between Ci and χ_s (**Fig. 5**). Understanding these physiological controls of χ_s
565 is essential for modeling its dynamic behaviour.

566

567 **Acknowledgments**

568 This study was supported by the National Natural Science Foundation of China
569 (41705130), Key Research Program of Frontier Sciences, CAS (QYZDB-SSW-
570 DQC019), the National Key R&D Program of China (2017YFC0210106), the Hundred
571 Talents Program, Chinese Academy of Sciences.

572

573

574 **References**

- 575 Akhtar, N., Yamaguchi, M., Inada, H., Hoshino, D., Kondo, T., Izuta, T., 2010. Effects
576 of ozone on growth, yield and leaf gas exchange rates of two Bangladeshi cultivars
577 of wheat (*Triticum aestivum* L.). Environ. Pollut. 158, 1763–1767.
- 578 Behera, S.N., Sharma, M., Aneja, V.P., Balasubramanian, R., 2013. Ammonia in the
579 atmosphere: a review on emission sources, atmospheric chemistry and deposition on
580 terrestrial bodies. Environ. Sci. Pollut. R. 20(11), 8092–8131.
- 581 Bertolini, T., Flechard, C.R., Fattore, F., Nicolini, G., Stefani, P., Materia, S., Valentini,

582 R., Vaglio L.G., Castaldi, S., 2016. DRY and BULK atmospheric nitrogen deposition
583 to a West-African humid forest exposed to terrestrial and oceanic sources. *Agr.*
584 *Forest Meteor.* 218–219, 184–195.

585 Cardoso-Vilhena, J., Barnes, J., 2001. Does nitrogen supply affect the response of
586 wheat (*Triticum aestivum* cv. Hanno) to the combination of elevated CO₂ and O₃? *J.*
587 *Exp. Bot.* 52, 1901–1911.

588 CLRTAR, 2015. Chapter 3: Mapping critical levels for vegetation. Manual on
589 methodologies and criteria for modelling and mapping critical loads & levels and air
590 pollution effects, risks and trends. Manual on Methodologies and Criteria for
591 Modelling and Mapping Critical Loads and Levels and Air Pollution Effects, Risks
592 and Trends. United Nations Economic Commission for Europe (UNECE)
593 Convention on Long-range Transboundary Air Pollution, Geneva
594 ([URL:http://www.icpmapping.org](http://www.icpmapping.org)).

595 Cooper, O.R., Parrish, D.D., Ziemke, J., Balashov, N.V., Cupeiro, M., Galbally, I.E.,
596 Gilge, S., Horowitz, L., Jensen, N.R., Lamarque, J.F., Naik, V., Oltmans, S.J.,
597 Schwab, J., Shindell, D.T., Thouret, V., Wang, Y., Zbinden, R.M., 2014. Global
598 distribution and trends of tropospheric ozone: An observation-based review.
599 *Elementa Science of the Anthropocene* 2, 000029, doi:
600 10.12952/journal.elementa.000029.

601 Du, E., Jiang, Y., Fang, J.Y., de Vries, W., 2014. Inorganic nitrogen deposition in
602 China's forests: Status and characteristics. *Atmos. Environ.* 98(98), 474–482.

603 Du, E., de Vries, W., Liu, X., Fang, J., Galloway, J. N., Jiang, Y., 2015. Spatial
604 boundary of urban 'acid islands' in southern China. *Sci. Rep.* 5, 12635.

605 Duyzer, J., Pilegaard, K., Simpson, D., Weststrate, H., Walton, S., 2005. A simple
606 model to estimate exchange rates of nitrogen dioxide between the atmosphere and
607 forests. *Biogeosciences Discuss.* 2, 1033–1065.

608 Erisman, J.W., Bleeker, A., Galloway, J., Sutton, M.S., 2007. Reduced nitrogen in
609 ecology and the environment. *Environ. Pollut.* 150(1), 140–149.

610 Feng, Z.Z., Wang, S.G., Szantoi, Z., Chen, S.A., Wang, X.K., 2010. Protection of
611 plants from ambient ozone by applications of ethylenediurea (EDU): A meta-analytic

612 review. *Environ. Pollut.* 158(10), 3236–3242.

613 Feng, Z.Z., Sun, J.S., Wan, W.X., Hu, E.Z., Calatayud, V., 2014. Evidence of
614 widespread ozone-induced visible injury on plants in Beijing, China. *Environ. Pollut.*
615 193(1), 296–301.

616 Feng, Z.Z., Wang, L., Pleijel, H., Zhu, J.G., Kobayashi, K., 2016. Differential effects
617 of ozone on photosynthesis of winter wheat among cultivars depend on antioxidative
618 enzymes rather than stomatal conductance. *Sci. Total Environ.* 572, 404–411.

619 Finnemann, J., Schjoerring, J.K., 1999. Translocation of NH_4^+ in oilseed rape plants in
620 relation to glutamine synthetase isogene expression and activity. *Physiol. Plantarum*
621 105, 469–477.

622 Flechard, C.R., Massad, R.S., Loubet, B., Personne, E., Simpson, D., Bash, J.O., Cooter,
623 E.J., Nemitz, E., Sutton, M.A., 2011. Advances in understanding, models and
624 parameterizations of biosphere-atmosphere ammonia exchange. *Biogeosciences*
625 10(7), 5183–5225.

626 Flechard, C. R., Massad, R. S., Loubet, B., Personne, E., Simpson, D., Bash, J. O.,
627 Cooter, E. J., Nemitz, E., Sutton, M. A., 2013. Advances in understanding, models
628 and parameterizations of biosphere-atmosphere ammonia exchange. *Biogeosciences*
629 10(7), 5183–5225.

630 Gao, F., Catalayud, V., Paoletti, E., Hoshika, Y., Feng, Z.Z., 2017. Water stress
631 mitigates the negative effects of ozone on photosynthesis and biomass in poplar plants.
632 *Environ. Pollut.* 230, 268–279.

633 Grignon, C., Sentenac, H., 1991. pH and ionic conditions in the apoplast. *Annu. Rev.*
634 *Plant Biol.* 42, 103–128.

635 Gu, B.J., Sutton, M.A., Chang, S.X., Ge, Y., Jie, C., 2014. Agricultural ammonia
636 emissions contribute to China's urban air pollution. *Front. Ecol. Environ.* 12(5), 265–
637 266.

638 Hansen, K., Sørensen, L.L., Hertel, O., Geels, C., Skjøth, C.A., Jensen, B., Boegh, E.,
639 2013. Ammonia emissions from deciduous forest after leaf fall. *Biogeosciences* 10,
640 4577–4589.

641 Hansen, K., Personne, E., Skjøth, C.A., Loubet, B., Ibrom, A., Jensen, R., Sørensen,

642 L.L., Boegh, E., 2017. Investigating sources of measured forest-atmosphere
643 ammonia fluxes using two-layer bi-directional modeling. *Agr. Forest Meteor.* 237–
644 238, 80–94.

645 Hanstein, S., Mattsson, M., Jaeger, H.-J., Schjoerring, J. K., 1999. Uptake and
646 utilization of atmospheric ammonia in three native Poaceae species: leaf
647 conductances, composition of apoplastic solution and interactions with root nitrogen
648 supply. *New Phytol.*, 141(1), 71–83.

649 Harmens, H., Hayes, F., Sharps, K., Mills, G., Calatayud, V., 2017. Leaf traits and
650 photosynthetic responses of *Betula pendula* saplings to a range of ground-level ozone
651 concentrations at a range of nitrogen loads. *J Plant Physiol.* 211, 42–52.

652 Herrmann, B., Mattsson, M., Jones, S. K., Cellier, P., Milford, C., Sutton, M. A.,
653 Schjoerring, J. K., Neftel, A., 2009. Vertical structure and diurnal variability of
654 ammonia exchange potential within an intensively managed grass canopy.
655 *Biogeosciences* 6(1), 15–23.

656 Hill, P.W., Raven, J.A., Loubet, B., Fowler, D., Sutton, M.A., 2001. Comparison of gas
657 exchange and bioassay determinations of the ammonia compensation point in *Luzula*
658 *sylvatica*, (Huds.) Gaud. *Plant Phys.* 125, 476–487.

659 Hill, P.W., Raven, J.A., Sutton, M.A., 2002. Leaf age-related differences in apoplastic
660 NH_4^+ concentration, pH and the NH_3 compensation point for a wild perennial. *J. Exp.*
661 *Bot.* 53(367), 277–286.

662 Hoffmann, B., Planker, R., Mengel, K., 1992. Measurements of pH in the apoplast of
663 sunflower leaves by means of fluorescence. *Physiol. Plantarum* 84, 146–153.

664 Hu, E.Z., Gao, F., Xin, Y., Jia, H.X., Li, K.H., Hu, J.J., Feng, Z.Z., 2015. Concentration-
665 and fluxbased ozone dose-response relationships for five poplar clones grown in
666 North China. *Environ. Pollut.* 207, 21–30.

667 Huppe, H.C., Turpin, D.H., 1994. Integration of carbon and nitrogen metabolism in
668 plant and algal cells. *Annu. Rev. Plant Biol.* 45(1), 577–607

669 Husted, S., Schjoerring, J. K., 1995. Apoplastic pH and Ammonium Concentration in
670 Leaves of *Brassica napus* L. *Plant Physiol.* 109(4), 1453–1460.

671 IPCC, 2013. *Climate Change 2007: The Physical Science Basis*. In *Contribution of*

672 Working Group I to the Fifth Assessment Report of the Intergovernmental Panel on
673 Climate Change. Intergovernmental Panel on Climate Change (eds Stocker T.F., Qin
674 D., Plattner G.K., Tignor M.M.B., Allen S.K., Boschung J., et al.), pp. 1552,
675 Cambridge University Press, Cambridge, United Kingdom and New York, NY, USA.
676 Kanakidou, M., Myriokefalitakis, S., Daskalakis, N., Fanourgakis, G., 2016. Past,
677 present, and future atmospheric nitrogen deposition. *J. Atmos. Sci.* 73 (5),
678 160303130433005.

679 Kosegarten, H., Englisch, G., 1994. Effect of various nitrogen forms on the pH in leaf
680 apoplast and on iron chlorosis of *Glycine max* L. *J. Plant Nutr. Soil Sc.* 157(6), 401–
681 405.

682 Kronzucker, H.J., Schjoerring, J.K., Erner, Y., Kirk, G.J.D., Siddiqi, M.Y., Glass,
683 A.D.M., 1998. Dynamic interactions between root NH_4^+ influx and long-distance N
684 translocation in rice [*Oryza sativa*]: Insights into feedback processes. *Plant Cell*
685 *Physiol.* 39(12): 1287–1293.

686 Li, P., Feng, Z.Z., Catalayud, V., Yuan, X.Y., Xu, Y.S., Paoletti, E., 2017. A meta-
687 analysis on growth, physiological, and biochemical responses of woody species to
688 ground-level ozone highlights the role of plant functional types. *Plant Cell Environ.*
689 40(10), 2369–2380.

690 Li, Y., Schichtel, B.A., Walker, J.T., Schwede, D.B., Chen, X., Lehmann, C.M.,
691 Puchalski, M.A., Gay, D.A., Collett, J.L., 2016. Increasing importance of deposition
692 of reduced nitrogen in the United States. *Proc. Natl. Acad. Sci. U.S.A.* 113 (21), 5874.

693 Lichtenthaler, H.K., 1987. [34] Chlorophylls and carotenoids: pigments of
694 photosynthetic biomembranes. *Methods Enzym.* 148, 350–382.

695 Liu, X.J., Song, L., He, C.E., Zhang, F.S., 2010. Nitrogen deposition as an important
696 nutrient from the environment and its impact on ecosystems in China. *J Arid Land*
697 2(2), 137–143.

698 Liu, X.J., Duan, L., Mo, J.M., Du, E.Z., Shen, J.L., Lu, X.K., Zhang, Y., Zhou, X.B.,
699 He, C.E., Zhang, F.S., 2011. Nitrogen deposition and its ecological impact in China:
700 an overview. *Environ. Pollut.* 159(10), 2251–2264.

701 Lohaus, G., Pennewiss, K., Sattelmacher, B., Hussmann, M., Muehling, K.H., 2001. Is

702 the infiltration–centrifugation technique appropriate for the isolation of apoplastic
703 fluid? A critical evaluation with different plant species. *Physiol. Plantarum* 111(4),
704 457–465.

705 Loubet, B., Milford, C., Hill, P.W., Tang, Y. S., Cellier, P., Sutton, M.A., 2002.
706 Seasonal variability of apoplastic NH_4^+ and pH in an intensively managed grassland.
707 *Plant Soil* 238(1), 97–110.

708 Massad, R.S., Loubet, B., Tuzet, A., Cellier, P., 2008. Relationship between ammonia
709 stomatal compensation point and nitrogen metabolism in arable crops: Current status
710 of knowledge and potential modelling approaches. *Environ. Pollut.* 154(3), 390–403.

711 Massad, R.S., Loubet, B., Tuzet, A., Autret, H., Cellier, P., 2009. Ammonia stomatal
712 compensation point of young oilseed rape leaves during dark/light cycles under
713 various nitrogen nutritions. *Agr. Ecosyst. Environ.* 133(3), 170–182.

714 Massad, R.S., Nemitz, E., Sutton, M.A., 2010. Review and parameterisation of bi-
715 directional ammonia exchange between vegetation and the atmosphere. *Atmos.*
716 *Chem. Phys.* 10(21), 10359–10386.

717 Mattsson, M., Schjoerring, J., 1996. Ammonia emission from young barley plants:
718 influence of N source, light/dark cycles and inhibition of glutamine synthetase. *J.*
719 *Exp. Bot.* 47(4), 477–484.

720 Mattsson, M., Husted, S., Schjoerring, J.K., 1998. Influence of nitrogen nutrition and
721 metabolism on ammonia volatilization in plants. *Nutr. Cycl. Agroecosys.* 51(1), 35–
722 40.

723 Mattsson, M., Schjoerring, J. K., 2003. Senescence-induced changes in apoplastic and
724 bulk tissue ammonia concentrations of ryegrass leaves. *New Phytol.* 160(3), 489–
725 499.

726 Mattsson, M., Herrmann, B., David, M., Loubet, B., Riedo, M., Theobald, M.R., Sutton,
727 M.A., Bruhn, D., Neftel, A., Schjoerring, J.K., 2009. Temporal variability in
728 bioassays of the stomatal ammonia compensation point in relation to plant and soil
729 nitrogen parameters in intensively managed grassland. *Biogeosciences* 6(2), 171–
730 179.

731 Mengel, K., Plänker, R., Hoffmann, B., 1994. Relationship between leaf apoplast pH

732 and iron chlorosis of sunflower (*Helianthus annuus*). *J. Plant Nutr.* 17(6),1053–
733 1065.

734 Neirynek, J. and Ceulemans, R., 2008. Bidirectional ammonia exchange above a mixed
735 coniferous forest. *Environ. Pollut.* 154, 424–438.

736 Nemitz, E., Flynn, M., Williams, P.I., Milford, C., Theobald, M.R., Blatter, A.,
737 Gallagher, M.W., Sutton, M.A., 2001. A relaxed eddy accumulation system for the
738 automated measurement of atmospheric ammonia fluxes. *Water Air Soil Pollut.*
739 *Focus* 1(5–6), 189–202.

740 Nielsen, K.H., Schjoerring, J.K., 1998. Regulation of apoplastic NH_4^+ concentration in
741 leaves of oilseed rape. *Plant Physiol.* 118(4), 1361–1368.

742 Pakeman, R.J., Alexander, J., Brooker, R., Cummins, R., Fielding, D., Gore, S.,
743 Hewison, R., Mitchell, R., Moore, E., Orford, K., 2016. Long-term impacts of
744 nitrogen deposition on coastal plant communities. *Environ. Pollut.* 212, 337–347.

745 Paoletti, E., Materassi, A., Fasano, G., Hoshika, Y., Carriero, G., Silaghi, D., Badea, O.,
746 2016. A new-generation 3D ozone FACE (Free Air Controlled Exposure). *Sci. Total*
747 *Environ.* 575, 1407–1414.

748 Pearson, J., Clough, E.C.M., Woodall, L.J., Havill, D.C., Zhang, X.-H., 1998.
749 Ammonia emissions to the atmosphere from leaves of wild plants and *Hordeum*
750 *vulgare* treated with methionine sulphoximine. *New Phytol.* 138, 37–48.

751 Personne, E., Tardy, F., Générmont, S., Decuq, C., Gueudet, J.C., Mascher, N., Durand,
752 B., Masson, S., Lauransot, M., Fléhard, C., Burkhardt J., Loubet B., 2015.
753 Investigating sources and sinks for ammonia exchanges between the atmosphere and
754 a wheat canopy following slurry application with trailing hose. *Agr. Forest Meteor.*
755 207, 11–23.

756 Peuke, A.D., Jeschke, W.D., Hartung, W., 1998. Foliar application of nitrate or
757 ammonium as sole nitrogen supply in *Ricinus communis*. II. The flows of cations,
758 chloride and abscisic acid. *New Phytol.* 140(4), 625–636.

759 Raven J.A., Farquhar G.D., 1989. Leaf apoplast pH estimation in *Phaseolus vulgaris*.
760 In: Dainty J, Michelis MI, MarrèE, Rasi-Caldogno F, eds. *Plant membrane transport:*
761 *the current position.* Amsterdam: Elsevier, 607–610.

762 Riedo, M., Milford, C., Schmid, M., Sutton, M.A., 2002. Coupling soil-plant -
763 atmosphere exchange of ammonia with ecosystem functioning in grasslands. *Ecol.*
764 *Model.* 158(1-2), 83–110.

765 Sattelmacher, B., 2001. The apoplast and its significance for plant mineral nutrition.
766 *New Phytol.* 149(2), 167–192.

767 Schjoerring, J.K., Mattsson, M., Husted, S., 1998. Physiological parameters controlling
768 plant-atmosphere ammonia exchange. *Atmos. Environ.* 32(3): 491-498.

769 Schjoerring, J.K., Husted, S.M.G., Nielsen, K., Finnemann, J. Matt, M., 2000.
770 Physiological regulation of plant-atmosphere ammonia exchange. *Plant Soil* 221(1),
771 95-102.

772 Schjoerring, J.K., Husted, S., Mack, G., Mattsson, M., 2002. The regulation of
773 ammonium translocation in plants. *J. Exp. Bot.* 53(370), 883–890.

774 Shang, B., Feng, Z.Z., Li, P., Yuan, X.Y., Xu, Y.S., Calatayud, V., 2017. Ozone
775 exposure and flux-based response relationships with photosynthesis, leaf morphology
776 and biomass in two poplar clones. *Sci. Total Environ* 603–604, 185–195.

777 Sutton, M.A., Schjoerring, J.K., Wyers, G.P., 1995. Plant atmosphere exchange of
778 ammonia. *Philos. T. Roy. Soc. S-A.* 351, 261–278.

779 Sutton, M.A., Nemitz, E., Milford, C., Campbell, C., Erisman, J.W., Hensen, A., Cellier,
780 P., David, M., Loubet, B., Personne, E., Schjoerring, J.K., Mattsson, M., Dorsey, J.R.,
781 Gallagher, M.W., Horvath, L., Weidinger, T., Meszaros, R., Dämmgen, U., Neftel,
782 A., Herrmann, B., Lehman, B.E., Flechard, C., Burkhardt, J., 2009. Dynamics of
783 ammonia exchange with cut grassland: synthesis of results and conclusions of the
784 GRAMINAE Integrated Experiment. *Biogeosciences* 6(12), 2907–2934.

785 The Royal Society, 2008. Ground-level ozone in the 21st century: future trends, impacts
786 and policy implications. *Science Policy Report 15/08.* The Royal Society, London.

787 Van Hove, L. W. A., Heeres, P., Bossen, M. E., 2002. The annual variation in stomatal
788 ammonia compensation point of rye grass (*Lolium perenne L.*) leaves in an
789 intensively managed grassland. *Atmos. Environ.* 36(18), 2965-2977.

790 Vet, R., Artz, R.S., Carou, S., Shaw, M., Ro, C.-U., Aas, W., Baker, A., Bowersox,
791 V.C., Dentener, F., Galy-Lacaux, C., Hou, A., Pienaar, J.J., Gillett, R., Cristina Forti,

792 M., Gromov, S., Hara, H., Khodzher, T., Mahowald, N.M., Nickovic, S., Rao, P.S.P.,
793 Reid, N.W., 2014. A globe assessment of precipitation, chemistry and deposition of
794 sulfur, nitrogen, sea salt, base cations, organic acids, acidity and pH, and phosphorus.
795 Atmos. Environ. 93 (3–4), 3–100.

796 Wang, L., Xu, Y.C., Schjoerring, J.K., 2011. Seasonal variation in ammonia
797 compensation point and nitrogen pools in beech leaves (*Fagus sylvatica*). Plant Soil
798 343 (1-2), 51–66.

799 Xu, W., Luo, X.S., Pan, Y.P., Zhang, L., Tang, A.H., Shen, J.L., Zhang, Y., Li, K.H.,
800 Wu, Q.H., Yang, D.W., Zhang, Y.Y., Xue, J., Li, W.Q., Li, Q.Q., Tang, L., Lu, S.H.,
801 Liang, T., Tong, Y.A., Liu, P., Zhang, Q., Xiong, Z.Q., Shi, X.J., Wu, L.H., Shi,
802 W.Q., Tian, K., Zhong, X.H., Shi, K., Tang, Q.Y., Zhang, L.J., Huang, J.L., He, C.E.,
803 Kuang, F.H., Zhu, B., Liu, H., Jin, X., Xin, Y.J., Shi, X.K., Du, E.Z., Dore, A.J.,
804 Tang, S., Collett, J.L., Goulding, K., Sun, Y.X., Ren, J., Zhang, F.S., Liu, X.J., 2015.
805 Quantifying atmospheric nitrogen deposition through a nationwide monitoring
806 network across China. Atmos. Chem. Phys. 15, 12345–12360.

807 Xu, W., Wu, Q.H., Liu, X.J., Tang, A.H., Dore, A., Heal, M., 2016. Characteristics of
808 ammonia, acid gases, and PM_{2.5} for three typical land-use types in the North China
809 Plain. Environ. Sci. Pollut. R. 23(2), 1158–1172.

810 Xu, W., Song, W., Zhang, Y., Liu, X., Zhang, L., Zhao, Y., Liu, D., Tang, A., Yang,
811 D., Wang, D., 2017. Air quality improvement in a megacity: implications from 2015
812 Beijing Parade Blue pollution control actions. Atmos. Chem. Phys. 17, 31–46.

813 Yuan, X.Y., Calatayud, V., Gao, F., Fares, S., Paoletti, E., Tian, Y., Feng, Z.Z., 2016.
814 Interaction of drought and ozone exposure on isoprene emission from extensively
815 cultivated poplar. Plant Cell Environ. 39(10):2276.

816 Zhang, L., Wright, P. L., Asman, W. A. H., 2010. Bi-directional air-surface exchange
817 of atmospheric ammonia – A review of measurements and a development of a big-
818 leaf model for applications in regional-scale air-quality models. J. Geophys. Res.,
819 115, D20310, doi:10.1029/2009JD013589.

820 Zhang, W.W., Feng, Z.Z., Wang, X.K., Niu, J.F., 2012. Responses of native
821 broadleaved woody species to elevated ozone in subtropical China. Environ. Pollut.

822 163(4), 149–157.

823 Zhao, Y., Zhang, L., Chen, Y.F., Liu, X.J., Xu, W., Pan, Y.P., Duan, L., 2017.

824 Atmospheric nitrogen deposition to China: a model analysis on nitrogen budget and
825 critical load exceedance. *Atmos. Environ.* 153, 32–40.

826

827

828

829

830

831

832

833

834

835

836

837 **Figure captions**

838 Figure 1. Effects of ozone (CF, charcoal-filtered ambient air, and E-O₃, elevated O₃)
839 and Nitrogen (N0, no N added, and N50, 50 kg N ha⁻¹ yr⁻¹) on light-saturated
840 photosynthesis (A_{sat}), stomatal conductance (g_s), intercellular CO₂ concentration (C_i)
841 and chlorophyll (Chl) content of hybrid poplar clone ‘546’ (*Populus deltoides* cv. 55/56
842 \times *P. deltoides* cv. *Imperial*). Data shown are the mean \pm standard deviation of three-
843 OTC measurements. The letters on top of the bars are based on the Tukey test across
844 the two measurements, with different letters indicating significantly different from each
845 other at $P < 0.05$.

846 Figure 2. Effects of ozone (CF, charcoal-filtered ambient air, and E-O₃, elevated O₃)
847 and Nitrogen (N0, no N added, and N50, 50 kg N ha⁻¹ yr⁻¹) on apoplastic NH₄⁺
848 concentration, tissue NH₄⁺ concentration, apoplastic pH and emission potential (Γ_s) of
849 hybrid poplar clone ‘546’ (*Populus deltoides* cv. 55/56 \times *P. deltoides* cv. *Imperial*). Data
850 shown are the mean \pm standard deviation of three-OTC measurements. The letters on
851 top of the bars are based on the Tukey test across the two measurements, with different

852 letters indicating significantly different from each other at $P < 0.05$.

853 Figure 3. Effects of ozone (CF, charcoal-filtered ambient air, and E-O₃, elevated O₃)
854 and Nitrogen (N0, no N added, and N50, 50 kg N ha⁻¹ yr⁻¹) on the stomatal
855 compensation point (χ_s)

856 Figure 4. Correlation between the stomatal compensation point (χ_s) and light-saturated
857 photosynthesis (A_{sat}), stomatal conductance (g_s), intercellular CO₂ concentration (C_i)
858 and chlorophyll (Chl) content across all ozone and nitrogen treatments. Green and red
859 dots represent charcoal-filtered ambient air (CF)*N0 (no N added), CF*N50 (50 kg N
860 ha⁻¹ yr⁻¹), elevated O₃ (E-O₃)*N0 and E-O₃*N50 treatment in July and August,
861 respectively. While ANCOVA did not show significant differences in the slope of the
862 regression lines for the relationships between the two measurement dates (i.e., July and
863 August), one single line is shown; otherwise, two lines are shown.

864 Figure 5. Correlations between apoplastic pH and light-saturated photosynthesis (A_{sat}),
865 chlorophyll (Chl) content, and intercellular CO₂ concentration (C_i), and correlation
866 between apoplastic NH₄⁺ concentration and leaf tissue NH₄⁺ concentration across all
867 ozone and nitrogen treatments. Green and red dots represent charcoal-filtered ambient
868 air (CF)*N0 (no N added), CF*N50 (50 kg N ha⁻¹ yr⁻¹), elevated O₃ (E-O₃)*N0 and E-
869 O₃*N50 treatment in July and August, respectively. While ANCOVA did not show
870 significant differences in the slope of the regression lines for the relationships between
871 the two measurement dates (i.e., July and August), one single line is shown; otherwise,
872 two lines are shown.

873 Figure 6. Actual forest distribution in China (a) (adopting from Li et al. (2017)) and
874 atmospheric NH₃ concentration over deciduous broadleaf forests in July (b) and August
875 (c) modeled using the GEOS-Chem model.

876

877

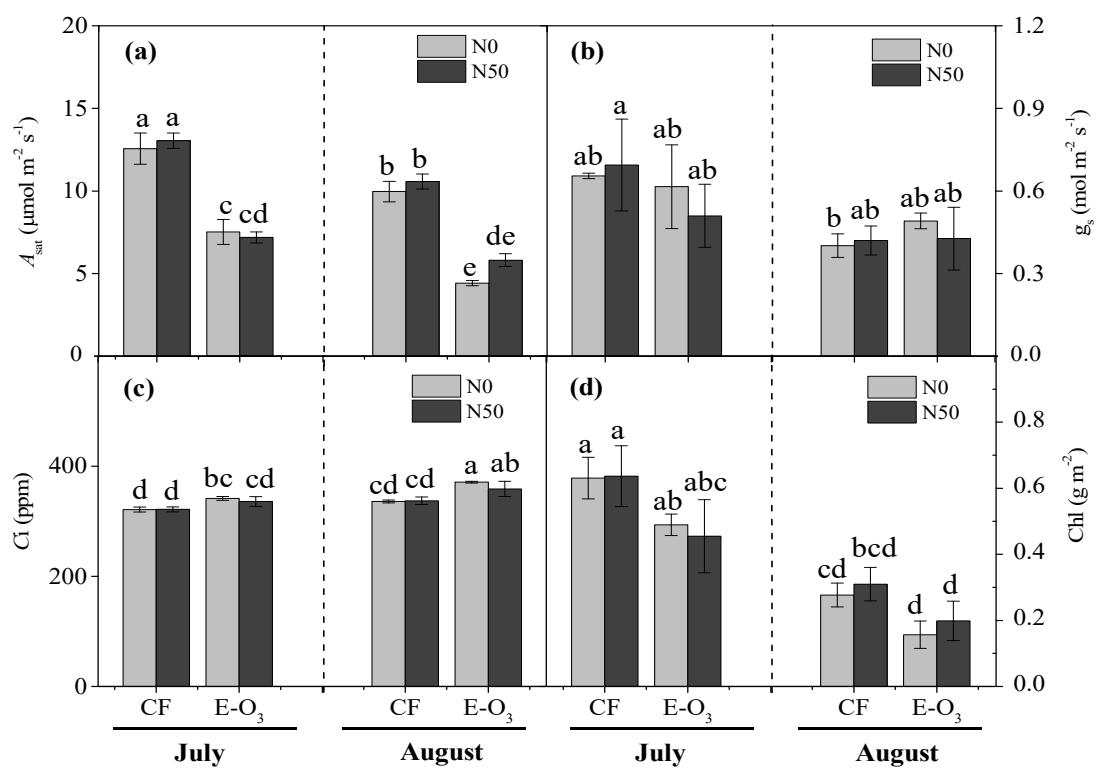
878

879

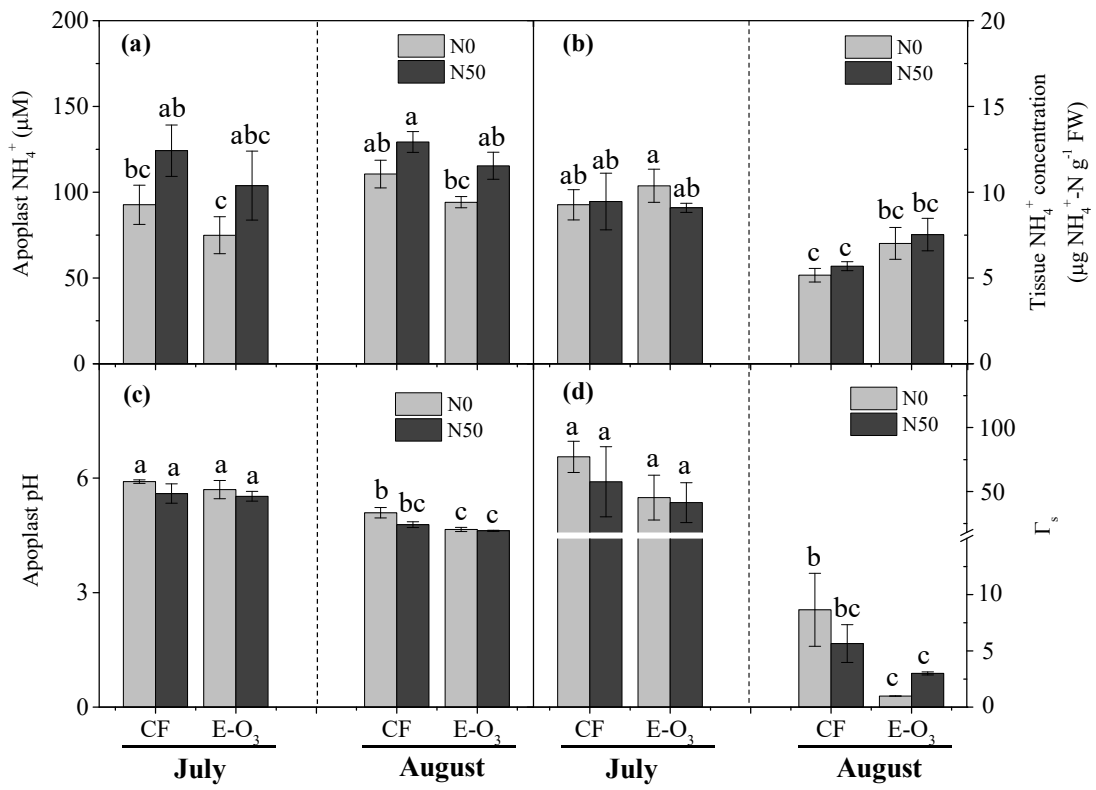
880

881

882
883
884
885
886
887
888
889
890
891
892
893
894
895
896
897 **Figure 1**

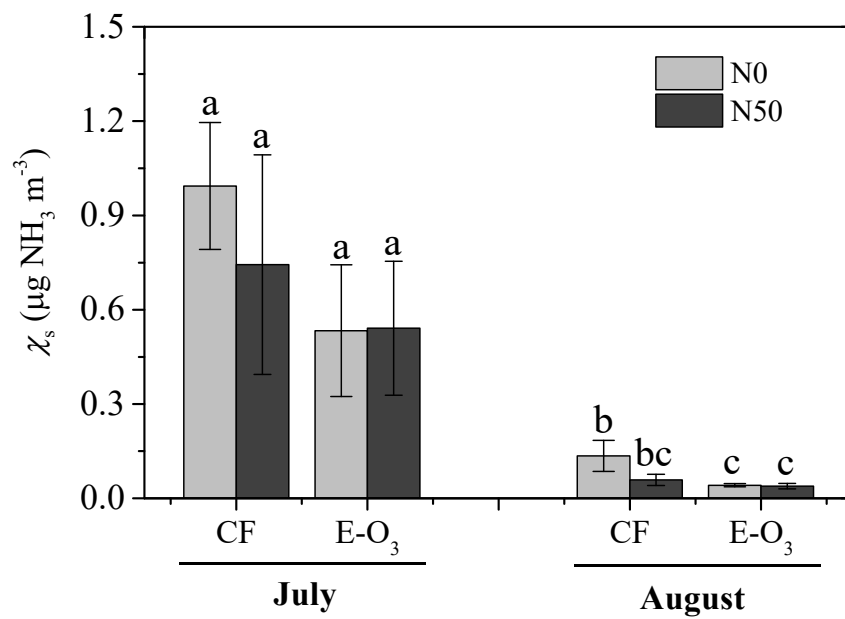


898
899 **Figure 2**



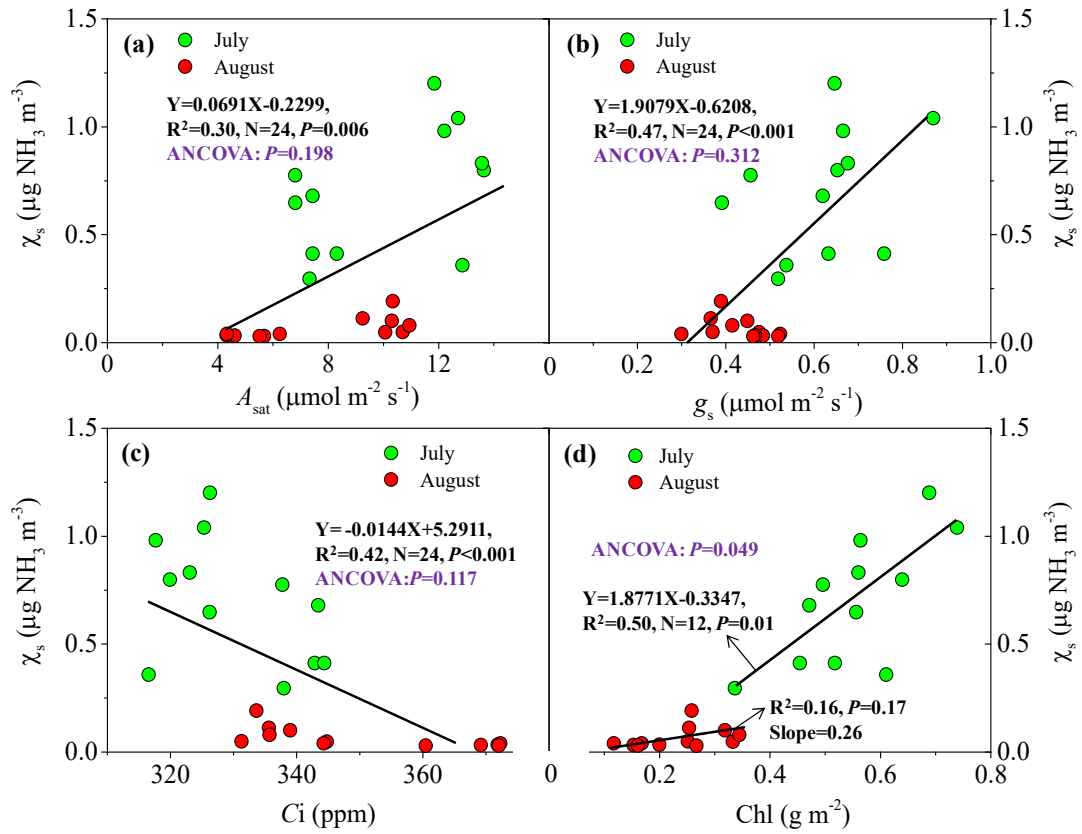
900
901
902
903
904
905

Figure 3



906
907

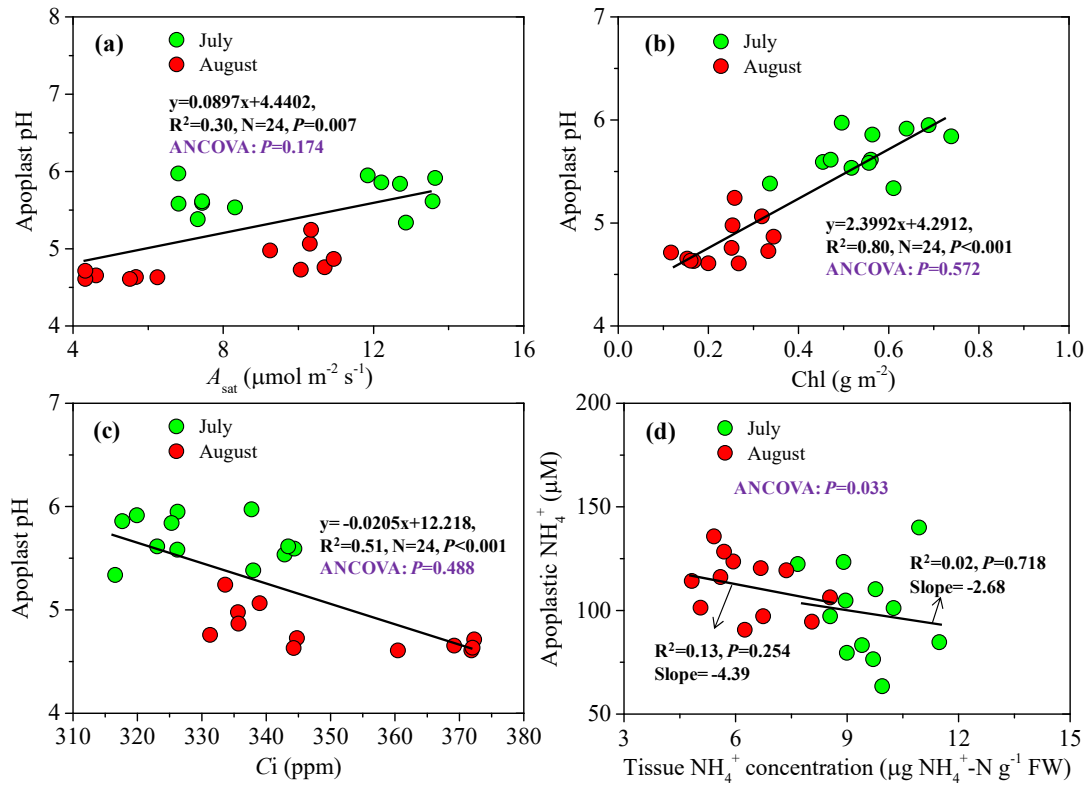
Figure 4



908

909

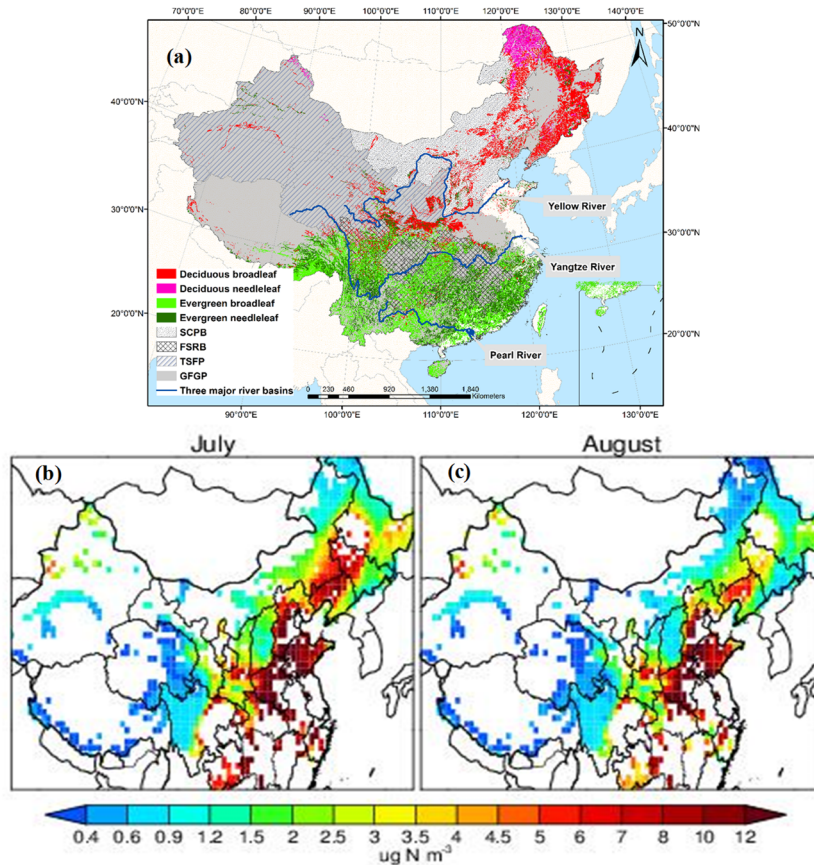
910 **Figure 5**



911

912

913 **Figure 6**



914

915 **Table 1.** ANOVA results (*P* values) for the individual effects of interactions of O₃ (CF
 916 and E-O₃), N (N0 and N50), and sampling data (July and August) on light-saturated rate
 917 of CO₂ assimilation (*A*_{sat}), stomatal conductance (*g*_s), intercellular CO₂ concentration
 918 (*C*_i), chlorophyll content (Chl), apoplastic pH, apoplastic NH₄⁺, leaf tissue NH₄⁺,
 919 potential emission (*Γ*_s), and stomatal compensation point (*χ*_s).

	O ₃	N	Date (D)	O ₃ *N	O ₃ *D	N*D	O ₃ *N*D
<i>A</i> _{sat}	<0.001	0.057	0.001	0.977	0.553	0.042	0.063
<i>g</i> _s	0.610	0.579	0.003	0.285	0.048	0.843	0.564
<i>C</i> _i	0.007	0.257	<0.001	0.192	0.002	0.404	0.295
Chl	0.006	0.612	0.001	0.727	0.527	0.375	0.658
Apoplast pH	0.015	0.018	<0.001	0.118	0.240	0.657	0.391
Apoplast NH ₄ ⁺	0.039	0.017	0.004	0.996	0.431	0.172	0.698
Leaf tissue NH ₄ ⁺	0.041	0.965	0.003	0.265	0.219	0.097	0.210
<i>Γ</i> _s	0.026	0.067	<0.001	0.062	0.318	0.777	0.369
<i>χ</i> _s	0.019	0.034	<0.001	0.032	0.203	0.322	0.337

920 CF: charcoal-filtered ambient air; E-O₃: elevated O₃; N0: no N added; N50: 50 kg N

921 $\text{ha}^{-1} \text{yr}^{-1}$; Statistically significant effects ($P < 0.05$) are marked in bold.

922